Boundary-Layer Meteorology (2024) 190:23
https://doi.org/10.1007/s10546-024-00867-9

RESEARCH ARTICLE

Local Similarity Theory as the Invariant Solution of the Governing Equations

Marta Wacławczyk[1] · Jun-Ichi Yano[2] · Grzegorz M. Florczyk[1]

Received: 11 December 2023 / Accepted: 29 March 2024 / Published online: 30 April 2024

Abstract
The present paper shows that local similarity theories, proposed for the strongly-stratified boundary layers, can be derived as invariant solutions defined under the Lie-group theory. A system truncated to the mean momentum and buoyancy equations is considered for this purpose. The study further suggests how similarity functions for the mean profiles are determined from the vertical fluxes, with a potential dependence on a measure of the anisotropy of the system. A time scale that is likely to characterize the transiency of a system is also identified as a non-dimensionalization factor.

Keywords Stably-stratified turbulence · Local similarity theory · Invariants · Lie symmetries

1 Introduction

Similarity theories are a key methodology for analyzing of flows in the atmospheric boundary layers (ABLs). They seek universal relationships between different physical variables describing the phenomenon, without explicitly solving the governing equations (Sorbjan 2016). The similarity theories rely on the so-called dimensional analyses (Barenblatt 1996), and identify the characteristic scales to non-dimensionalize the physical variables, which fit universal curves. The first and most celebrated similarity theory of ABLs was proposed by Monin and Obukhov (1954). Those authors introduced the Obukhov length scale, L, based on the surface momentum and heat fluxes to non-dimensionalize the height, z, (Obukhov 1948).

✉ Marta Wacławczyk
Marta.Waclawczyk@fuw.edu.pl

Jun-Ichi Yano
jiy.gfder@gmail.com

Grzegorz M. Florczyk
grzegorz.florczyk@fuw.edu.pl

[1] Faculty of Physics, Institute of Geophysics, University of Warsaw, Warsaw, Poland

[2] CNRM, UMR3589 (CNRS), Météo France, 31057 Toulouse Cedex, France

The standard Monin–Obukhov similarity theory (MOST) is believed to work well in the case that is homogeneous in time and space, with relatively weak stratifications. The assumed forms of the similarity functions suggest that the gradient Richardson number should tend to a constant, critical value, $Ri_{cr} \approx 0.2$, in the limit of the strong stratification. However, as the stratification further increases, turbulence tends to locally collapse, and as a result, intermittent transitions between turbulent and non-turbulent states are observed (Allouche et al. 2022; Ansorge and Mellado 2014). This modifies the scaling of mean wind and temperature, and the Richardson number no longer levels off at Ri_{cr}.

Due to deviations of the experimental results from the MOST predictions, different theories were developed: Zilitinkevich and Calanca (2000), Zilitinkevich and Esau (2005), and Zilitinkevich and Esau (2007) introduced additional scales characterizing effect of the Earth's rotation and the stability of free-flow. Grachev et al. (2015) considered Dougherty-Ozmidov scale, which is constructed from the turbulence kinetic energy dissipation rate. Generalization of MOST accounting for the turbulence anisotropy in ABL was proposed recently by Stiperski and Calaf (2023).

Of particular relevance for this work is the formulation of the 'local similarity theory' by Nieuswtadt (1984): instead of the surface values of fluxes, this theory uses their local values (i.e. measured at height z) to estimate the length scale, $\Lambda(z)$, with $\Lambda(z) \approx L$ when it is close enough to the surface. This approach was further advanced by Sorbjan (1989), who assumed more general relationships for the variation of fluxes with height.

As alternatives to the local MOST, Sorbjan (2006, 2016) proposed gradient-based similarity theories, which express the fluxes and other statistical quantities as functions of the Richardson number, Ri. These alternative formulations have advantages, over the flux-based MOST approach, of describing the weak turbulence regimes better without invoking a critical Richardson number.

This work derives the local similarity theories of a form closely following those by Sorbjan (2006, 2016), directly from the system of governing equations, instead of dimensional analyses. A similar problem was addressed by Yano and Wacławczyk (2022) with the use of the technique of non-dimensionalization (cf., Yano and Bonazzola 2009). Here, we alternatively adopt a concept of symmetries, defined by the transformations of variables that do not change the form of governing equations. The symmetries lead to invariant solutions of the considered system. By analyzing a system of governing equations as a starting point, functional relations between different variables can be derived methodologically.

The symmetry analysis can also reveal relations between the variables, that were previously unknown. For example, general formulas are derived for mean profiles as functions of flux-related variables. In this manner, the symmetry method can provide broader perspectives on similarity theories, by identifying assumptions behind them in a systematic way.

The notion of 'invariance' was already remarked by Monin and Obukhov (1954), although the symmetry transformations were not explicitly invoked therein. Symmetry-based methods were previously used in numerous works to obtain solutions for neutrally stratified flows in different flow configurations, e.g., Oberlack (2001), Oberlack et al. (2022), Avsarkisov et al. (2014), Sadeghi et al. (2021). Among others, the logarithmic law of the wall was derived in Oberlack and Rosteck (2010). Ji and She (2021) used symmetry-based generalised dilation approach to derive expression for the mixing length in the atmospheric surface layer. The Lie symmetries for the surface layer with non-zero buoyancy were considered by Yano and Wacławczyk (2023), in which the logarithmic and linear profiles for the mean wind and temperature were discussed.

In this paper, the local similarity theories are derived as functions of Lie group invariants of ABL flows. The local Obukhov length naturally appears in these solutions, as a combination

of invariants, rather than as an externally introduced length scale. Moreover, the obtained general solutions contain dependencies on time, or alternatively, on a measure of anisotropy of the flow. Significantly, the derived solutions generalize the gradient-based similarity theories of Sorbjan (2016): the former reduces to the latter, when the Richardson number remains constant with height.

We consider the two distinct regions of the ABL: the outer layer, where fluxes depend on the boundary layer height, h, and the surface layer, where no external length scale governs the turbulent transports. We especially take into account an intermittency parameter, which indicates a degree that a given flow can be presented as a sum of two different contributions, e.g., turbulent and laminar, but also e.g., logarithmic and linear. When this parameter is set to zero, a solution reduces to the linear forms for mean wind and buoyancy. On the other hand, when it is non-zero, it accounts for the variability of the Richardson number at strong stratifications.

Seeking the universal forms of non-dimensionalized gradients of the mean wind, ϕ_m, and mean buoyancy, ϕ_h, which are independent of the local values of the intermittency parameter, we arrive, under certain assumptions, at the relations $\phi_m \sim \xi/Ri\,G$ and $\phi_h \sim \xi/Ri\,G^2$, where $\xi = z/L$ and the Prandtl number, G, is a function of the aspect ratio of the Reynolds stresses, which we further interpret as a measure of anisotropy of the flow. On the other hand, the analysis of experimental data from the Surface Heat Budget of the Arctic Ocean (SHEBA) experiment (Persson et al. 2002) suggests more general forms, $\phi_m \sim (\xi/Ri\,G)^p$ and $\phi_h \sim (\xi/Ri\,G^2)^q$ with $p = 1/3$ and $q = -1$ for very weak stratifications, and $p = 1$, $q = 1$ for strong stratifications. Furthermore, we estimate value of the intermittency parameter based on the SHEBA data.

The paper is organized as follows: Sect. 2 describes the local similarity theories in details. The symmetry methods are introduced in Sects. 3 and 4. Invariants of ABL flows are discussed in Sect. 5. Sections 6 and 7 are devoted to the derivation of the invariant solutions in the outer and surface layer, respectively. Data analyses are performed in Sect. 8, followed by conclusions and perspectives.

2 Overview of the Local Similarity Theories

Processes in the atmospheric boundary layer are governed by a closed set of partial differential equations. However, due to the complexity of the processes, these equations cannot yet be solved numerically for real-world configurations. Alternatives are the similarity theories, which propose certain rescaling of the variables, that collapse the measurements collected during various experiments onto single universal curves.

The MOST expresses the turbulence moments as functions of the stability parameter, $\xi = z/L$, where:

$$L = -\frac{1}{\kappa}\frac{|\overline{uw}_0|^{3/2}}{\overline{wb}_0} = \frac{1}{\kappa}\frac{u_*^2}{b_*}, \tag{1}$$

is the Obukhov length, and $\overline{uw}_0$ and $\overline{wb}_0$ are the surface values of momentum and buoyancy fluxes, respectively. The buoyancy, b, is defined as:

$$b = g(\theta - \theta_0(z))/\theta_m, \tag{2}$$

where $\theta - \theta_0(z)$ denotes deviation of the potential temperature, θ, from a steady reference state and θ_m is a vertical average. In MOST, the scales, L, $u_* = |\overline{uw}_0|^{1/2}$, and $u_* b_* =$

$-\overline{wb}_0$, represent the external conditions. The similarity functions, on the other hand, express universal dependencies of turbulence moments on stability parameter ξ. In particular, Monin and Obukhov (1954) proposed to express the non-dimensional mean wind and buoyancy gradients in the stable BL as (cf., Foken 2006):

$$\frac{\kappa z}{u_*} S = \phi_m(\xi) = 1 + 5\,\xi, \tag{3a}$$

$$\frac{\kappa z}{b_*} N^2 = \phi_h(\xi) = 1 + 5\,\xi, \tag{3b}$$

where $S = \mathrm{d}\bar{u}/\mathrm{d}z$ is the mean wind shear, and $N^2 = \mathrm{d}\bar{b}/\mathrm{d}z$ is the square of the Brunt–Väisälä frequency. Businger et al. (1971) further elaborated the formulas, and proposed $\phi_m = 1{+}4.7\xi$ and $\phi_h = 0.74 + 4.7\xi$.

The question of whether the MOST correctly describes turbulence statistics in stable boundary layers (SBL), especially under weak turbulence, is subject of ongoing debate. For weak stratifications, the MOST is believed to work well within the surface layer, over which the fluxes are approximately constant with height. Nieuswtadt (1984) reformulated MOST by introducing the local length scale:

$$\Lambda = -\frac{1}{\kappa}\frac{|\overline{uw}|^{3/2}}{\overline{wb}}, \tag{4}$$

as a similarity scale. In this reformulation, the equations describing relationships between dimensionless combinations of variables were measured at the same height.

In the outer layer, Nieuswtadt (1984) presented the momentum and buoyancy fluxes as functions of z/h, where h was the boundary layer height, and more specifically, suggested the relations $\overline{uw} = u_*^2(1 - z/h)^{3/2}$ and $\overline{wb} = u_* b_* (1 - z/h)$ based on observations. Sorbjan (1989) proposed further generalizations of the Nieuwstadt's approach by assuming the following profiles of turbulent fluxes:

$$\overline{uw} = \overline{uw}_0 \left(1 - \frac{z}{h}\right)^p, \quad \overline{wb} = \overline{wb}_0 \left(1 - \frac{z}{h}\right)^q, \tag{5}$$

where $p \geq q$.

The local scaling is valid only for strong, continuous turbulence, for the subcritical values of the flux Richardson number, Ri, and, additionally, under the assumption that Ri is constant with height (Sorbjan 2006). These conditions are not fulfilled in very stable ABLs, which consist of layered structures, representing a 'sporadic' turbulence intermittency. To overcome deficiencies of local similarity theory, Sorbjan (2006, 2016) proposed the alternative, gradient-based scalings:

$$u_N = L_N N, \quad b_N = L_N N^2, \quad L_N = l, \tag{6}$$

where l is a length scale, which can be defined either as the mixing length $l = \kappa z$ (explicit scaling) or as a function of turbulence moments (implicit scaling); u_N and b_N are the velocity and buoyancy scales constructed by using L_N and the Brunt–Väisälä frequency N. For the implicit scaling, the following combination can be considered (Sorbjan 2016):

$$l = \frac{(\overline{w^2})^{1/2}}{N}. \tag{7}$$

In the gradient-based formulations, the Richardson number, Ri, or the flux-based Richardson number, R_f, (rather than z/Λ) plays a role of stability parameter. These parameters are defined by:

$$Ri = \frac{N^2}{S^2}, \quad R_f = \frac{\overline{wb}}{\overline{uw}\, S}. \tag{8}$$

It immediately follows from Eqs. (3a), (3b), and (4) that:

$$Ri = \frac{z}{\Lambda} \frac{\phi_h}{\phi_m^2}. \tag{9}$$

Thus, Ri becomes a function of z/Λ, and as a result, Ri can be used as a vertical coordinate of the system in place of z/Λ.

Based on this observation, Sorbjan (2012) formulated a generalized form of the similarity theory assuming:

$$\frac{l}{u_*} S = \psi_m(Ri), \quad \frac{l}{b_*} N^2 = \psi_h(Ri). \tag{10}$$

With $l = \kappa z$ and expressing Ri explicitly as a function of z/Λ by Eq. (9), the local MOST formulation is recovered. Moreover, Sorbjan (2016) postulated that non-dimensionalized fluxes can be presented as functions of Ri:

$$\frac{\overline{uw}}{u_N^2} = \mathcal{G}(Ri), \quad \frac{\overline{wb}}{u_N b_N} = \mathcal{H}(Ri). \tag{11}$$

Alternatively, non-dimensionalized turbulent fluxes as functions of R_f were considered by Łobocki (2013), Łobocki and Porretta-Tomaszewska (2021). Those authors determined the forms of $\mathcal{G}$ and $\mathcal{H}$ based on the Mellor–Yamada turbulence-closure model. Advantage of the gradient-based scaling is that u_N is less sensitive to sampling errors and the choice of averaging window than u_*. Moreover, spurious self-correlations are avoided, when fluxes are presented as functions of Ri.

3 Symmetry Analysis

3.1 Introduction

To derive local similarity theories from a system of governing equations, we first need to identify the transformations of the variables that leave the equations unchanged, i.e. transformations that do not affect the physics of a given system. These transformations are called the symmetries of the governing equations; the concept was first introduced by a Norwegian mathematician Sophus Lie in the second half of the nineteenth century. In the following, we apply symmetry analyses for deriving these transformations to the two examples: Monin–Obukhov arguments on invariant functions and by analyzing symmetries of the diffusion equation.

3.2 Monin–Obukhov

Even though the Lie symmetries were not explicitly mentioned by Monin and Obukhov (1954), those authors used a similar concept, namely the concept of invariant. Let the variables z and t transform into a new set of independent variables z^* and t^*. Also, a dependent variable, say $\theta(z, t)$, is transformed to $\theta^*(z^*, t^*)$. An invariant is a function $C(\theta, z, t)$, which preserves its form when it is written in terms of the new variables:

$$C(\theta, z, t) = C(\theta^*, z^*, t^*).$$

Monin and Obukhov (1954) argued that statistical characteristics of the relative movements in a stream are invariant with respect to the following similarity transformations:

$$x^* = \lambda x, \quad y^* = \lambda y, \quad z^* = \lambda z, \quad t^* = \lambda t. \tag{12}$$

It was also implicitly assumed that the system is conserved by the translation of the mean wind velocity:

$$\bar{u}^* = \bar{u} + \bar{u}_0. \tag{13}$$

Consequently, Monin and Obukhov (1954) considered difference of velocities at two different heights. In this case the translation shifts cancel, and:

$$\bar{u}^*(z_2^*) - \bar{u}^*(z_1^*) = \bar{u}(z_2) - \bar{u}(z_1), \tag{14}$$

is an invariant with respect to all the above transformations. As argued by those authors, the non-dimensional magnitude is a function of both z_1 and z_2, but because it must also be invariant under the scaling (12), it must be a function of the ratio z_2/z_1:

$$\frac{\bar{u}(z_2) - \bar{u}(z_1)}{u_*} = f\left(\frac{z_2}{z_1}\right). \tag{15}$$

Monin and Obukhov (1954) used the form (15) to derive the logarithmic solution for the mean wind.

3.3 Diffusion Equation

We briefly present the main concepts of the Lie group analysis, taking as an example, the one-dimensional heat equation:

$$\frac{\partial \theta}{\partial t} = \frac{\partial^2 \theta}{\partial z^2}, \tag{16}$$

with the initial condition $\theta(z, 0) = \delta(z)$.

It can easily be verified that this equation remains unchanged under the transformations of θ, z and t into:

$$z^* = \lambda z, \quad t^* = \lambda^2 t, \quad \theta^* = \theta/\lambda, \tag{17}$$

where $\lambda > 0$ is a constant, i.e.,(17) are symmetry transformations, which represent symmetries of the problem (16). It can be shown that they form a mathematical object called a group.

3.4 Group and Invariant Transformations

Mathematically, a group consists of a non-empty set and a pre-defined operation, in which a third element, that is created by combining any two arbitrary elements by the given operation, must also be an element of this set. Additionally required conditions are: the operation must be associative; an identity element must exist; and every element must have an inverse.

All the properties of the group are satisfied by the transformation (17). It can be demonstrated by presenting (17) in the exponential form $z^* = \lambda z = \mathrm{e}^{\epsilon} z$, where $\epsilon \in \mathrm{R}$. Combination of two transformations:

$$z^* = \mathrm{e}^{\epsilon_1}\left(\mathrm{e}^{\epsilon_2} z\right), \tag{18}$$

is a new transformation:

$$z^* = \mathrm{e}^{\epsilon_1+\epsilon_2} z = \mathrm{e}^{\epsilon} z. \tag{19}$$

The unitary element of the transformation is obtained by setting $\epsilon = 0$. The inverse element is derived by replacing ϵ by $-\epsilon$, so that:

$$z^* = \mathrm{e}^{\epsilon}\mathrm{e}^{-\epsilon} z = z. \tag{20}$$

The associativity property is also satisfied by $z^* = (\mathrm{e}^{\epsilon_1}\mathrm{e}^{\epsilon_2})\mathrm{e}^{\epsilon_3} z = \mathrm{e}^{\epsilon_1}(\mathrm{e}^{\epsilon_2}\mathrm{e}^{\epsilon_3})z$.

The Lie group analysis is a method of determining Lie symmetry transformations of a given differential equation system. This, in turn, allows us to derive invariants and invariant solutions. Details of the Lie group analysis are beyond the scope of this paper, and an interested reader is referred to textbooks, e.g. Bluman and Kumei (1989). Also computer algebra systems can be used to identify all symmetries of a given, closed system of equations. The next important step is a derivation of invariant solutions from a given set of symmetry transformations. This study focuses on this second step.

For this purpose, we introduce infinitesimal forms by expanding the global transformation forms, z^*, t^* and θ^*, in the Taylor series around $\epsilon = 0$:

$$\begin{aligned} z^* &= z + \left.\frac{\mathrm{d}z^*}{\mathrm{d}\epsilon}\right|_{\epsilon=0} \epsilon + \mathcal{O}(\epsilon^2), \quad t^* = t + \left.\frac{\mathrm{d}t^*}{\mathrm{d}\epsilon}\right|_{\epsilon=0} \epsilon + \mathcal{O}(\epsilon^2), \\ \theta^* &= \theta + \left.\frac{\mathrm{d}\theta^*}{\mathrm{d}\epsilon}\right|_{\epsilon=0} \epsilon + \mathcal{O}(\epsilon^2); \end{aligned} \tag{21}$$

The first-order derivatives at $\epsilon = 0$ are called "infinitesimals", and will be denoted by ξ_z, ξ_t and η. As the Lie's theorem states, the global forms of transformations, z^*, t^* and θ^*, are obtained by integrating the infinitesimal forms:

$$\frac{\mathrm{d}z^*}{\mathrm{d}\epsilon} = \xi_z(z^*, t^*, \theta^*), \quad \frac{\mathrm{d}t^*}{\mathrm{d}\epsilon} = \xi_t(z^*, t^*, \theta^*), \quad \frac{\mathrm{d}\theta^*}{\mathrm{d}\epsilon} = \eta(z^*, t^*, \theta^*), \tag{22}$$

with the initial conditions $z^* = z$, $t^* = t$, and $\theta^* = \theta$ at $\epsilon = 0$. In this manner, the infinitesimal and global forms become equivalent.

The infinitesimal generator, X, of the transformations for the heat equation is defined by:

$$\mathrm{X} = \xi_z(z, t, \theta)\frac{\partial}{\partial z} + \xi_t(z, t, \theta)\frac{\partial}{\partial t} + \eta(z, t, \theta)\frac{\partial}{\partial \theta}. \tag{23}$$

The solution $\theta = \Theta(z, t)$ is an invariant solution of the heat equation (16), if and only if it satisfies equation:

$$\mathrm{X}\left(\theta - \Theta(z, t)\right) = \xi_z(z, t, \theta)\frac{\partial \Theta}{\partial z} + \xi_t(z, t, \theta)\frac{\partial \Theta}{\partial t} + \eta(z, t, \theta) = 0, \tag{24}$$

and solves Eq. (16).

The condition (24) can be solved by a method of characteristics, solving the corresponding characteristic equation:

$$\frac{\mathrm{d}z}{\xi_z(z, t, \theta)} = \frac{\mathrm{d}t}{\xi_t(z, t, \theta)} = \frac{\mathrm{d}\theta}{\eta(z, t, \theta)}. \tag{25}$$

As an example, let us consider the scaling transformations (17), and rewrite them as $z^* = \mathrm{e}^{\epsilon} z$, $t^* = \mathrm{e}^{2\epsilon}\, t$, $\theta^* = \mathrm{e}^{-\epsilon}\theta$. Infinitesimal forms of these transformations are, as defined by Eq. (21),

$$z^* = z + \xi_z \epsilon + \mathcal{O}(\epsilon^2) = z + z\epsilon + \mathcal{O}(\epsilon^2), \tag{26a}$$

$$t^* = t + \xi_t \epsilon + \mathcal{O}(\epsilon^2) = t + 2t\epsilon + \mathcal{O}(\epsilon^2), \tag{26b}$$

$$\theta^* = \theta + \eta\epsilon + \mathcal{O}(\epsilon^2) = \theta - \theta\epsilon + \mathcal{O}(\epsilon^2), \tag{26c}$$

and the corresponding characteristic equation (25) reads:

$$\frac{\mathrm{d}z}{z} = \frac{\mathrm{d}t}{2t} = \frac{\mathrm{d}\theta}{-\theta}. \tag{27}$$

3.5 Invariant Solutions

Solving for the two equalities in Eq. (27), we find two invariants X and C:

$$X = \frac{z}{\sqrt{t}}, \quad C = \sqrt{t}\,\theta, \tag{28}$$

which remain unchanged when written in new variables (17). The relations (28) correspond e.g. to characteristic curves obtained by Riehman's method in wave dynamics (Lighthill 1978). The solution of Eq. (27) is given implicitly by the invariant form:

$$C = F(X), \quad \text{hence} \quad \theta = \frac{1}{\sqrt{t}} F\left(\frac{z}{\sqrt{t}}\right), \tag{29}$$

where F is an arbitrary function. Here, an invariant, X, from now on, plays a role of an independent variable of the system.

Substituting (29) into the heat equation (16), we obtain a reduced equation with one independent variable X,

$$2F'' + C_1 F' + F = 0, \tag{30}$$

which determines the form of the function F.

Note that invariance under the scaling groups is linked to the dimensional analysis and the Buckingham Pi-theorem (Buckingham 1914). As argued by Bluman and Kumei (1989), if a dimensional analysis leads to a reduction of the number of independent variables, then such a reduction is always possible through invariance under scalings; however, the opposite is not always true. In this manner, the invariance of variables under scaling groups is considered a generalization of the dimensional analyses.

The main goal of this work is to present a solution of a boundary-layer system as a function of invariant variables. Here, considered dependent variables are: the mean velocity and buoyancy gradients, S, N^2, as well as the mean pressure $\overline{p}$, fluxes $\overline{uw}$, $\overline{wb}$ and the variance $\overline{w^2}$. As a consequence, the local similarity theory is directly derived from the set of governing equations in an invariant form as given by Eq. (29).

4 Lie Group Analysis of the Governing Equations

4.1 Governing Equations

We consider flows in the atmospheric boundary layer, governed by the Navier–Stokes system under the Boussinesq approximation and in the inviscid limit. We perform ensemble averaging of the prognostic equations, and as a result, any physical variable, ϕ, is decomposed into mean and fluctuation, i.e.,$\phi = \overline{\phi} + \phi'$, as usually considered in turbulence studies. However, by following Oberlack et al. (2022), we consider ensemble averages of total quantities, e.g. $\overline{uw}$

rather than of fluctuations, $\overline{u'w'}$, because the equation system becomes linear in terms of those total averages. In some cases, the averages of instantaneous variables will be identical to the correlations of fluctuations, e.g. if $\overline{w} = 0$, we have $\overline{uw} = \overline{u'w'}$ and $\overline{wb} = \overline{w'b'}$. However, the same does not automatically apply to the other statistics. Furthermore, we assume that horizontal gradients of velocity moments are smaller than the vertical gradient by an order of magnitude, and that the Coriolis force is balanced by the horizontal pressure gradients, thus by subtracting the geostrophic-pressure component, the Coriolis force no longer plays an explicit role. In the following, the horizontal coordinate, x, is taken as the direction of the mean wind.

Under those assumptions, the governing equation system reads:

$$\frac{\partial \overline{u}}{\partial t} + \frac{\partial \overline{uw}}{\partial z} = 0, \tag{31a}$$

$$\frac{\partial \overline{w^2}}{\partial z} = -\frac{1}{\rho_0}\frac{\partial \overline{p}}{\partial z} + \bar{b}, \tag{31b}$$

$$\frac{\partial \overline{b}}{\partial t} + \frac{\partial \overline{wb}}{\partial z} = 0, \tag{31c}$$

where ρ_0 is a constant mean density, and p is the pressure.

The system (31a)–(31c) is unclosed, because there are more depedent variables than an available number of equations. It is well known in the boundary-layer meteorology that for solving this differential equation system, a certain closure is required. Yet, it is still possible to consistently identify the transformation rules to all the dependent variables as well as coordinates (independent variables) of the system that conserves the given equation set (Oberlack and Rosteck 2010). From those identified transformation rules, it is also possible to derive the invariant solutions of the system. Importantly, those obtained invariant solutions still constitute special solutions of a given system, even though the system is underdetermined.[1]

4.2 Groups of Transformations: List

The purpose of this subsection is to present the symmetry transformations satisfied by this system one by one with the considerations of their characteristics. We consider the symmetries of the Navier–Stokes equations with zero viscosity (cf., Pukhnachev 1972), and, additionally, the invariance under scaling and groups of translations of an infinite hierarchy of equations for moments (Oberlack and Rosteck 2010).

Equations (31a)–(31c) are invariant under the time and space translations:

$$t^* = t + t_0, \tag{32a}$$

$$\mathbf{x}^* = \mathbf{x} + \mathbf{f}(t), \quad \bar{\mathbf{u}}^* = \bar{\mathbf{u}} + \frac{\mathrm{d}\mathbf{f}(t)}{\mathrm{d}t}, \quad \bar{p}^* = \bar{p} - \mathbf{x}\cdot\frac{\mathrm{d}^2\mathbf{f}(t)}{\mathrm{d}t^2}, \tag{32b}$$

where $\mathbf{u} = (u, v, w)$, $\mathbf{x} = (x, y, z)$, and $\mathbf{f}(t)$ is an arbitrary vector function of time. It is invariant furthermore, under a rotations on the x-y plane, under pressure translations

[1] Formal mathematical issues yet still remain due to the more dependent variables than available equations. These issues may be avoided by treating an excess of dependent variables as *external functions*: those external functions must also be transformed in a similar manner as proper dependent variables. To elucidate those mathematical subtleties, Frewer et al. (2015) suggest to call the invariances for these external functions to be "equivalence" rather than "symmetry" transformations.

$\bar{p}^* = \bar{p} + g(t)$ with $g(t)$ an arbitrary function of time, as well as under the translations:

$$\bar{b}^* = \bar{b} + b_0, \quad \bar{p}^* = \bar{p} + z\rho_0 b_0. \tag{32c}$$

The two further scaling-group symmetries are included for the considerations:

$$t^* = t, \quad z^* = \mathrm{e}^{a_z} z, \quad \bar{u}^* = \mathrm{e}^{a_z}\bar{u}, \quad \bar{b}^* = \mathrm{e}^{a_z}\bar{b}, \quad \overline{p}^* = \mathrm{e}^{2a_z}\overline{p}, \tag{32d}$$
$$\overline{uw}^* = \mathrm{e}^{2a_z}\overline{uw}, \quad \overline{w^2}^* = \mathrm{e}^{2a_z}\overline{w^2}, \quad \overline{wb}^* = \mathrm{e}^{2a_z}\overline{wb},$$
$$t^* = \mathrm{e}^{a_t} t, \quad z^* = z, \quad \bar{u}^* = \mathrm{e}^{-a_t}\bar{u}, \quad \bar{b}^* = \mathrm{e}^{-2a_t}\bar{b}, \quad \overline{p}^* = \mathrm{e}^{-2a_t}\overline{p},$$
$$\overline{uw}^* = \mathrm{e}^{-2a_t}\overline{uw}, \quad \overline{w^2}^* = \mathrm{e}^{-2a_t}\overline{w^2}, \quad \overline{wb}^* = \mathrm{e}^{-3a_t}\overline{wb}, \tag{32e}$$

They will become particularly important for the derivation of scaling laws in the following.

When the buoyancy $\bar{b}$ can be neglected in the momentum equation (31b), e.g., under the neutral stratifications, an additional, independent scaling group for the buoyancy exists:

$$\bar{b}^* = \mathrm{e}^{a_b}\bar{b}. \tag{32f}$$

Refer to the discussions in the Appendix of Yano and Wacławczyk (2023) for more details.

As shown by Oberlack and Rosteck (2010), Eqs. (31a)–(31c) are invariant under additional translations due to their linearities: see also Wacławczyk et al. (2017). Generally, arbitrary known solutions of a linear system can be added to the variables by a linear superposition principle. However, we will only include translations by a constant in the following, because this form of translation for the mean velocity leads to the logarithmic solution identified by Monin and Obukhov (1954):

$$\overline{u}^* = \overline{u} + u_0, \quad \overline{b}^* = \overline{b} + b_0, \tag{33a}$$
$$\overline{uw}^* = \overline{uw} + uw_0, \quad \overline{wb}^* = \overline{wb} + wb_0, \quad \overline{w^2}^* = \overline{w^2} + w_0^2. \tag{33b}$$

A further statistical scaling group is identified in Khujadze and Oberlack (2004), Oberlack and Rosteck (2010) :

$$t^* = t, \quad z^* = z, \quad \bar{u}^* = \mathrm{e}^{a_s}\bar{u}, \quad \bar{b}^* = \mathrm{e}^{a_s}\bar{b}, \quad \overline{p}^* = \mathrm{e}^{a_s}\overline{p},$$
$$\overline{uw}^* = \mathrm{e}^{a_s}\overline{uw}, \quad \overline{w^2}^* = \mathrm{e}^{a_s}\overline{w^2}, \quad \overline{wb}^* = \mathrm{e}^{a_s}\overline{wb}. \tag{33c}$$

The invariance of the system (31a)–(31c) under the above transformations can be verified in a straightforward manner by direct substitutions. Transformations (33b) and (33c) have no correspondence in symmetries of the instantaneous velocity u and buoyancy b. For this reason, they are referred "statistical groups". The statistical scaling basically represents the fact that if the set of variables $\overline{u}$, $\overline{uw}$, $\overline{wb}$, $\overline{w^2}$, $\overline{p}$, $\overline{b}$ solves equations (31a)–(31c), then, due to their linearity, also does the set $\gamma\overline{u}$, $\gamma\overline{uw}$, $\gamma\overline{wb}$, $\gamma\overline{w^2}$, $\gamma\overline{p}$, $\gamma\overline{b}$ where:

$$\gamma = \mathrm{e}^{a_s}. \tag{34}$$

Wacławczyk et al. (2014) related the statistical scaling to the phenomenon of intermittency, understood as alternating occurence of laminar and turbulent flows. If we consider two different types of solutions of the equations (e.g. turbulent and laminar), denoting them by indices 1 and 2, a solution can be presented by a weighted sum of conditional statistics:

$$\overline{u}^* = \gamma\overline{u}_1 + (1-\gamma)\overline{u}_2, \quad \overline{b}^* = \gamma\overline{b}_1 + (1-\gamma)\overline{b}_2, \tag{35}$$

where $0 \leq \gamma \leq 1$ becomes an intermittency factor, if $a_s \leq 0$. γ is equal to the unity when the flow is fully turbulent, and vanishes when it is purely laminar. Because a_s is restricted to $a_s < 0$, the transformations (33c) form a semi-group.

Such a representation is linked to observations in very stable atmospheric boundary layers. As discussed by Allouche et al. (2022), the analysis in the intermittent regime cannot rely on bulk statistics, but may require conditional analysis. More generally, conditional statistics with indices 1 and 2 could refer to some limit cases, e.g.,a logarithmic function in neutral limit and a linear in the strongly stratified limit. The final solution can be represented as a weighted sum of these two limiting solutions.

Finally, when the Coriolis force is taken into account, the rotation, time scaling, and the statistical scaling group are modified to a more complex form, (cf., Rosteck 2014). It is left for a future study to consider these modifications. Here, we assume that the statistics are not influenced by the Earth's rotation, although for large stratifications this assumption may be too strong. In this work, horizontal transports are also neglected. This simplification does not affect the scaling symmetries (32d)–(32e), which are the same as in the underlying Navier–Stokes system. Furthermore, the invariance due to the statistical scaling group (33c) is a property of equations for moments in their general form, i.e. with the horizontal transport terms (cf., Oberlack and Rosteck 2010).

5 Invariants of Boundary-Layer Flows

5.1 Characteristic System

In deriving the invariants of the boundary-layer flows, we take into account the time translation symmetry (32a) and the space translation (32b), assuming that $\mathbf{f}(t) = \mathbf{x}_0$ is a constant vector, the scaling groups (32d)–(32e), as well as the statistical scaling and translations (33b), (33c). Consequently, we obtain the following characteristic system:

$$\begin{aligned}
\frac{\mathrm{d}t}{a_t(t-t_0)} &= \frac{\mathrm{d}z}{a_z(z-z_0)} = \frac{\mathrm{d}\overline{wb}}{(2a_z-3a_t+a_s)(\overline{wb}-wb_0)} = \\
\frac{\mathrm{d}\overline{uw}}{(2a_z-2a_t+a_s)(\overline{uw}-uw_0)} &= \frac{\mathrm{d}w^2}{(2a_z-2a_t+a_s)(\overline{w^2}-w_0^2)} = \\
\frac{\mathrm{d}\bar{b}}{(a_z-2a_t+a_s)(\bar{b}-b_0)} &= \frac{\mathrm{d}\bar{u}}{(a_z-a_t+a_s)(\bar{u}-u_0)} = \\
&= \frac{\mathrm{d}\bar{p}}{(2a_z-2a_t+a_s)(\bar{p}-p_0-zb_0\rho_0\alpha)},
\end{aligned} \tag{36}$$

where $\alpha = (a_z - 2a_t + a_s)/(2a_z - 2a_t + a_s)$. Solving the system (36), we obtain the 7 invariants:

$$t - t_0 = X_t\,|z-z_0|^{\beta} \tag{37a}$$

$$\bar{u} - u_0 = C_u\,|z-z_0|^{1-\beta+\chi}\,, \tag{37b}$$

$$\bar{b} - b_0 = C_b\,|z-z_0|^{1-2\beta+\chi}\,, \tag{37c}$$

$$\frac{\bar{p}}{\rho_0} - \frac{p_0}{\rho_0} = C_p\,|z-z_0|^{2-2\beta+\chi} - \frac{b_0\alpha[z_0-(2-2\beta+\chi)z]}{1-2\beta+\chi}, \tag{37d}$$

$$\overline{uw} - uw_0 = C_1\,|z-z_0|^{2-2\beta+\chi}\,, \tag{37e}$$

$$\overline{w^2} - w_0^2 = C_2\,|z-z_0|^{2-2\beta+\chi}\,, \tag{37f}$$

$$\overline{wb} - wb_0 = C_3\,|z-z_0|^{2-3\beta+\chi}\,, \tag{37g}$$

where:

$$\beta = a_t/a_z, \quad \text{and} \quad \chi = a_s/a_z. \tag{37h}$$

5.2 Invariant Solutions

The invariants, C_u, C_p, C_b, C_1, C_2 and C_3 are functions of the new variable X_t, introduced by Eq. (37a), so that the invariant solutions (29) are generated as:

$$C_u = F(X_t), \quad C_p = G(X_t), \quad C_b = H(X_t), \tag{38a}$$

$$C_1 = C_1(X_t), \quad C_2 = C_2(X_t), \quad C_3 = C_3(X_t). \tag{38b}$$

After introducing these invariants into the system (31a–31c), the relations between C_u, C_b, C_p and remaining invariants can be derived.

In the following, we analyze the invariant solutions in the outer and surface layers of ABL separately: we expect that the statistics in the outer layer are influenced by the boundary layer height, h, but not the statistics of the surface layer.

6 Local Similarity: Outer Layer

6.1 Invariants

The constant z_0 in Eqs. (37a)–(37g) can be chosen in various ways, depending on the flow configuration. For the outer layer, we assume that $z_0 = h$, and that $u_0 = \bar{u}(h)$ and $b_0 = \bar{b}(h)$ play the roles of the velocity and buoyancy scales. With this choice, the heat and momentum fluxes change with the height as proposed by Sorbjan (1989), cf., his Eqs. (5). These forms are obtained as invariants by setting $z_0 = h$ in Eqs. (37a)–(37g). Then, the fluxes read:

$$\overline{uw} = C_1(X_t)\left(1 - \frac{z}{h}\right)^{2-2\beta+\chi}, \tag{39a}$$

$$\overline{w^2} = C_2(X_t)\left(1 - \frac{z}{h}\right)^{2-2\beta+\chi}, \tag{39b}$$

$$\overline{wb} = C_3(X_t)\left(1 - \frac{z}{h}\right)^{2-3\beta+\chi}. \tag{39c}$$

Those invariants can be rearranged to more convenient forms:

$$S = \frac{\partial \bar{u}}{\partial z} = \tilde{C}_u(X_t)\left(1 - \frac{z}{h}\right)^{\chi-\beta}, \tag{40a}$$

$$N^2 = \frac{\partial \bar{b}}{\partial z} = \tilde{C}_b(X_t)\left(1 - \frac{z}{h}\right)^{\chi-2\beta}, \tag{40b}$$

$$\frac{\overline{uw}}{\overline{w^2}} = \frac{C_1(X_t)}{C_2(X_t)} = f(X_t), \tag{40c}$$

$$\frac{\overline{wb}}{\overline{uw}}\left(1 - \frac{z}{h}\right)^{\beta} = \frac{C_3(X_t)}{C_1(X_t)} = g(X_t), \tag{40d}$$

$$\frac{\overline{wb}}{\overline{uw}}(t - t_0) = \frac{C_3(X_t)X_t}{C_1(X_t)} = q(X_t). \tag{40e}$$

Here, we have skipped the expression for the pressure, which is usually not considered as a part of similarity theories. Equations (40a) and (40b) together with formulas (40c)–(40e) lead

to local similarity formulas as going to be shown below. The ratios of fluxes in Eqs. (40c)–(40e) become functions of X_t. Moreover, the ratio C_3/C_1 from Eq. (40d) can be rearranged as follows:

$$\frac{C_3(X_t)}{C_1(X_t)} = -\sqrt{|\overline{uw}|}\frac{\overline{wb}}{|\overline{uw}|^{3/2}}\left(1-\frac{z}{h}\right)^{\beta} = \frac{\sqrt{|\overline{uw}|}}{\kappa\Lambda}\left(1-\frac{z}{h}\right)^{\beta}. \tag{41}$$

Remarkably, in Eq. (41), we find the local Obukhov length, Λ, defined in Eq. (4), which is one of the possible local length scales suggested in the local similarity theories (Nieuswtadt 1984). The ratio between the buoyancy and momentum fluxes is also found in Eq. (40e) as a factor to non-dimensionalize the time. All invariants can additionally depend on the characteristic scales of the system: h, u_0 and b_0 when needed for dimensional consistency.

6.2 Similarity Solutions

To derive formulas for S and N^2 in terms of fluxes, we substitute the factor $(1-z/h)^{\beta}$ calculated from Eq. (41) into Eqs. (40a) and (40b). We also assume that relations (40c) and (40e) can be inverted over a time interval, $\Delta t = t - t_0$, so that:

$$\frac{u_0}{h}X_t = f^{-1}\left(\frac{\overline{uw}}{\overline{w^2}}\right), \quad \frac{u_0}{h}X_t = q^{-1}\left(\frac{\overline{wb}}{\overline{uw}}(t-t_0)\right), \tag{42}$$

where the factor u_0/h has been included for the dimensional consistency. We take into account the first from relations (42). With this we obtain:

$$S = \frac{\sqrt{|\overline{uw}|}}{\kappa\Lambda}\left(1-\frac{z}{h}\right)^{\chi} F\left(\frac{|\overline{uw}|}{\overline{w^2}}\right), \tag{43a}$$

$$N^2 = -\frac{\overline{wb}}{\sqrt{|\overline{uw}|}}\frac{1}{\kappa\Lambda}\left(1-\frac{z}{h}\right)^{\chi} H\left(\frac{|\overline{uw}|}{\overline{w^2}}\right). \tag{43b}$$

In addition to the local Obukhov length Λ, S and N^2 also depend on a height-dependent prefactor, $(1-z/h)^{\chi}$ and the non-dimensional parameter, $|\overline{uw}|/\overline{w^2}$ through the similarity functions, F and H. Alternatively, F and H can be written as functions of the non-dimensional time, $(t-t_0)\overline{wb}/\overline{uw}$. In this manner, standard similarity solutions for the shear, S, and the stratification, N, are obtained formally under a quasi-stationary state as invariant solutions. Yet, it is worthwhile to note a crucial role played by a time-dependent characteristic, X_t, in deriving these quasi-stationary solutions; it further suggests that a weak transiency of the system, represented by X_t, plays a crucial role in determining those standard quasi-stationary state of the boundary layer.

The parameter, $|\overline{uw}|/\overline{w^2}$, can be interpreted as an aspect ratio of turbulent eddies in anisotropic flows. Stiperski et al. (2021) and Stiperski and Calaf (2023) suggest that departure of the scaling from the MOST is strongly correlated to the anisotropy of the Reynolds stress tensor. Some studies propose additional dependencies representing degrees of turbulence to the similarity functions under strong stratifications. For example, Klipp and Mahrt (2004) introduce a vertical-velocity variance threshold to filter out weak turbulence regimes. The analysis here points out more objectively that $|\overline{uw}|/\overline{w^2}$ is an additional dependent variable that characterizes the similarity functions.

The non-dimensional time, $(t-t_0)\,\overline{wb}/\overline{uw}$, represents a time dependence of the similarity functions for the mean wind shear and the stratification. We expect that the transiency

characterized by this non-dimensional time becomes important under strong stratifications. Importantly, the time is non-dimensionalized by the scale, $\overline{uw}/\overline{wb}$, thus a frequency distribution of $\overline{uw}/\overline{wb}$ should reveal the actual characteristic time scales of the system.

6.3 Richardson and Prandtl Numbers

As an important direct consequence from Eqs. (43a) and (43b), we derive the Richardson number as:

$$Ri = \frac{N^2}{S^2} = \left(1 - \frac{z}{h}\right)^{-\chi} \frac{H}{F^2}. \tag{44}$$

By inverting the above relation, $\overline{uw}/\overline{w^2}$ is extracted into:

$$\frac{|\overline{uw}|}{\overline{w^2}} = \mathcal{G}\left[Ri\left(1 - \frac{z}{h}\right)^{\chi}\right], \tag{45}$$

where $\mathcal{G}$ is a function obtained by an inversion. Furthermore, by introducing the definitions of the local non-dimensional functions ϕ_h and ϕ_m into Eqs. (43a) and (43b), we obtain:

$$\phi_m = \frac{\kappa z}{\sqrt{|\overline{uw}|}} S = \frac{z}{\Lambda}\left(1 - \frac{z}{h}\right)^{\chi} F, \tag{46a}$$

$$\phi_h = \kappa z \frac{\sqrt{|\overline{uw}|}}{-\overline{wb}} N^2 = \frac{z}{\Lambda}\left(1 - \frac{z}{h}\right)^{\chi} H. \tag{46b}$$

It follows from these two relations that the turbulent Prandtl number, $Pr_t = \phi_h/\phi_m$, is not a constant, but is a function of the non-dimensional ratio $|\overline{uw}|/\overline{w^2}$, or the non-dimensionalized time i.e.,

$$Pr_t = \frac{\phi_h}{\phi_m} = \frac{H}{F} \neq const. \tag{47}$$

A standard similarity theory for the surface layer predicts that the universal functions, ϕ_m and ϕ_h, are linear in their argument $\xi = z/L$ for weak stratifications. If we assume the same for the local similarity, i.e. that ϕ_m and ϕ_h are proportional to z/Λ, it then follows that the turbulent Prandtl number should be constant. Here, the derived solutions (46a, 46b) and (47) predict the deviations from those predictions in the outer layer.

6.4 Relations to the Gradient-Based Similarity Theory

Equation (45) with the dependence on Ri suggests a link to the Sorbjan's gradient-based similarity theory (cf., Sorbjan 2006, 2010, 2016). We now examine under what conditions the derived relationships reduce to this theory.

For this purpose, we adopt the scales $u_N^2 = \overline{w^2}$ and $b_N = u_N N$ defined by Eqs. (6) and (7). The relation (45) defined in the previous subsection already presents the momentum flux, $\overline{uw}$, non-dimensionalized by the scale u_N:

$$|\overline{uw}| = u_N^2 \mathcal{G}\left[Ri\left(1 - \frac{z}{h}\right)^{\chi}\right]. \tag{48}$$

To derive a formula for the buoyancy flux, we replace the ratio C_3/C_1 defined in Eq. (40d) by the ratio C_3/C_2:

$$\frac{C_3}{C_2} = \frac{\overline{wb}}{\overline{w^2}} \left(1 - \frac{z}{h}\right)^{\beta} = \frac{\overline{wb}}{u_N^2} \left(1 - \frac{z}{h}\right)^{\beta}, \tag{49}$$

and rewrite Eq. (43b) as:

$$N^2 = \frac{\overline{wb}^2}{u_N^4} \left(1 - \frac{z}{h}\right)^{\chi} H\left(\frac{|\overline{uw}|}{u_N^2}\right). \tag{50}$$

Applying the square root on (50) and after some rearrangements, we obtain:

$$\overline{wb} = N u_N^2 \left(1 - \frac{z}{h}\right)^{-\chi/2} \mathcal{H}\left[Ri \left(1 - \frac{z}{h}\right)^{\chi}\right], \tag{51}$$

where we have also replaced the first argument of the function H in Eq. (50) by taking into account of Eq. (48). Finally, when $\chi = 0$, Eqs. (48) and (51) become functions of Ri only, as predicted by Sorbjan (2016), cf., Eq. (11):

$$\overline{uw} = u_N \mathcal{G}(Ri), \quad \overline{wb} = N\overline{w^2}\mathcal{H}(Ri) = b_N u_N \mathcal{H}(Ri). \tag{52}$$

7 Local Similarity: Surface Layer

The surface layer is a region adjacent to the Earth's surface, where turbulent fluxes are believed to remain approximately constant with height. In this layer, we can assume that the statistics are not influenced by the boundary layer height, h, except for the case with strong stratifications. A local similarity theory can be derived from the given symmetries, but by proceeding differently: instead of h, the characteristic surface roughness, d, is introduced as an external length.

By deriving a local similarity from the given symmetries, the Obukhov length enters the solution as a combination of invariants, but this time only in the limit of the weak stratification when the local Obukhov length is approximately equal to its surface value.

7.1 Neutral Stratification

A region adjacent to the Earth's surface is affected by the surface roughness with the characteristic length, d. On the other hand, the statistics at higher altitudes are affected by another length scale—the boundary layer height, h. We assume that between these two regions, there exists a transition layer, where turbulent transport is affected neither by d nor h. We will hence expect that the gradient of velocity as well as the fluxes in the transition layer will not depend on d. Under the neutral stratification this requirement leads to the logarithmic solution. Logarithmic solution for near-wall flows was derived by Oberlack (2001) and Oberlack and Rosteck (2010) based on the symmetries of Navier–Stokes and statistical scaling and translation groups. Here, we first address the arguments of Monin and Obukhov (1954), who stated that the statistical characteristics of the relative movements in the neutral ABL are invariant with respect to space and time scaling prescribed by Eqs. (12). Their transformations for space and time are written in the global form, with $\lambda = \mathrm{e}^{a_z} = \mathrm{e}^{a_t}$. Hence, these transformations are equivalent to setting $a_z = a_t$, thus $\beta = 1$. The invariance of the relative

movements is further obtained by setting $a_s = 0$. It follows that, instead of Eq. (36), we consider the following reduced characteristic system for velocity statistics:

$$\frac{\mathrm{d}t}{a_z(t-t_0)} = \frac{\mathrm{d}z/d}{a_z(z-z_0)/d} = \frac{\mathrm{d}\bar{u}}{-\tilde{u}_0} = \frac{\mathrm{d}\overline{uw}}{0} = \frac{\mathrm{d}\overline{w^2}}{0}, \tag{53}$$

where we have defined $\tilde{u}_0 = \bar{u}_0/(a_z - a_t + a_s)$. As $\bar{u}_0$ is an arbitrary constant, we can assume that $\bar{u}_0/(a_z - a_t + a_s)$ remains finite in the limit of $a_z - a_t + a_s \to 0$. We also assume the zero translational constants, $uw_0 = 0$ and $w_0^2 = 0$, as suggested by division by zero in the last two terms. Furthermore, we have introduced d as an external length scale. Solving Eq. (53), we obtain the 4 invariants, C_u, C_1, C_2 and X_t, which express a logarithmic profile for the mean velocity:

$$\begin{aligned} \bar{u} &= \frac{-\bar{u}_0}{a_z} \ln \frac{(z-z_0)}{d} + C_u(X_t), \\ \overline{uw} &= C_1(X_t), \quad \overline{w^2} = C_2(X_t), \quad X_t = \frac{(t-t_0)d}{z-z_0}. \end{aligned} \tag{54}$$

The translation coefficient, z_0, can be interpreted as the zero-plane displacement height. Here, for the sake of our own self-consistency, the notations, d and z_0, are other way round from those commonly-adopted in the atmospheric boundary-layer literature. We now choose the constant $-u_0/a_z = u_*/\kappa$, and assume stationarity so that C_u, C_1 and C_2 do not depend on X_t. We further set $C_u = \mathcal{C}u_*$ with $\mathcal{C}$ a constant.

Under these assumptions, the logarithmic profile reduces to:

$$\bar{u} = \frac{u_*}{\kappa} \ln \left[\frac{(z-z_0)}{d} \right] + \mathcal{C}u_*. \tag{55}$$

Change of the surface roughness, d, produces a shift of the mean velocity, although the velocity gradient does not explicitly depend on d. The fluxes, $\overline{uw}$ and $\overline{w^2}$, do not depend on d, either, by assuming both C_1 and C_2 are constants. These conclusions are compatible with a standard assumption of constant (in time and space) fluxes in the surface layer, i.e.,$\overline{uw} = \overline{uw}_0 = -u_*^2$ and $\overline{w^2} = \overline{w^2}_0$.

We use the analogous arguments to solve a hyperbolic system for the buoyancy, taking into account of the additional symmetry (32f), that holds under the neutral stratifications. Thus,

$$\overline{wb} = \overline{wb}_0, \tag{56}$$

$$\bar{b} = \frac{b_*}{\kappa} \ln \left[\frac{(z-z_0)}{d} \right] + \mathcal{C}'b_*, \tag{57}$$

with $a_b = 0$, $a_s = 0$ and $a_t = a_z$, where $\mathcal{C}'$ is another constant.

Alternatively, we can consider the case with non-zero translational constants $uw_0 \neq 0$ and $w_0^2 \neq 0$ in the system Eq. (53). These choices lead to logarithmic solutions for the fluxes, as observed by e.g., for the variance and higher-order statistics of longitudinal velocity (Katul et al. 2016) and for $\overline{uw}$ in case of strong accelerations (Araya et al. 2015).

7.2 Stratified Flows

The presence of non-zero buoyancy in the momentum equations leads to a two-way coupling between the velocity and the buoyancy. As a result, the transformation (32f) is further constrained by an additional condition $a_b = a_z - 2a_t$, as discussed in Yano and Wacławczyk

(2023), and transformations of $\bar{b}$ are described by Eqs. (32d)–(32e). The fluxes will be constant in time and with height under the condition $a_t = a_z = a_s = 0$ and non-zero translations of space, mean wind and mean buoyancy in Eq. (36). Thus, the mean wind and buoyancy follow the linear profiles. With $\beta = 0$ and $\chi < 0$, the similarity functions increases more slowly with height. This was observed by Grachev et al. (2013), who found $\phi_m \sim \xi^{0.3}$. After removing data with $Ri > 0.2$ and $R_f > 0.2$, Grachev et al. (2013) concluded that the remaining results follow the MOST predictions very closely. This indicates a local collapse of turbulence at a very large stratification, leading to a significant departure from the MOST prediction.

Invariant solutions in the surface layer can be derived from the invariants (37a)–(37g) in the following manner. Unlike the outer-layer scaling in Sect. 6, the shift, z_0, is no longer related to any external length scale, and it can be assumed small. To arrive at the similarity solutions with the local Obukhov length, Λ, as before, we rearrange these coefficients as follows:

$$S = \tilde{C}_u (z - z_0)^{\chi-\beta}, \quad N^2 = \tilde{C}_b (z - z_0)^{\chi-2\beta}, \tag{58a}$$

$$C_1 = \overline{uw}' (z - z_0)^{2\beta-2-\chi}, \tag{58b}$$

$$\frac{C_1}{C_2} = \frac{\overline{uw}'}{w^{2'}}, \tag{58c}$$

$$\frac{C_3}{C_1} = \frac{\overline{wb}'}{\overline{uw}'} (z - z_0)^{\beta}, \tag{58d}$$

$$X_t \frac{C_3}{C_1} = (t - t_0) \frac{\overline{wb}'}{\overline{uw}'}, \tag{58e}$$

where the prime indices suggest deviations of fluxes from the surface values:

$$\overline{uw}' = \overline{uw} - \overline{uw}_0, \tag{59a}$$

$$\overline{wb}' = \overline{wb} - \overline{wb}_0, \tag{59b}$$

$$\overline{w^2}' = \overline{w^2} - \overline{w^2}_0. \tag{59c}$$

The invariant relations (58a)–(58e) can be deduced in analogous manner as in the outer layer, as presented in Sect. 6.2, with a major difference of the mean profiles being represented in terms of the flux perturbations defined by Eqs. (59a)–(59c). The results are rather unintuitive, and full implications are still to be fully investigated.

Alternatively, Eqs. (58b)–(58e) can be presented in terms of the vertical derivatives of fluxes or their gradients, assuming that the time dependence is weak. Thus,

$$\frac{C_1}{C_2} = \frac{\mathrm{d}\overline{uw}}{\mathrm{d}\overline{w^2}}, \tag{60a}$$

$$\frac{C_3}{C_1} = \frac{\mathrm{d}\overline{wb}}{\mathrm{d}\overline{uw}} (z - z_0)^{\beta}, \tag{60b}$$

$$X_t \frac{C_3}{C_1} = (t - t_0) \frac{\mathrm{d}\overline{wb}}{\mathrm{d}\overline{uw}}. \tag{60c}$$

Even though relations (60a)–(60c) contain gradients rather than the fluxes, under certain conditions there may exist a relationship between the gradients and the Obukhov length, Λ. To see this, first recall the definition of the local Obukhov length, Λ, given by (4), and assume that this length remains approximately constant in the surface layer $\Lambda \approx L$ so that

its differential is close to zero:

$$-\mathrm{d}\Lambda = \mathrm{d}\left[\frac{|\overline{uw}|^{3/2}}{\overline{wb}}\right] = \frac{3}{2}\frac{(|\overline{uw}|)^{1/2}}{\overline{wb}}\mathrm{d}|\overline{uw}| - \frac{(|\overline{uw}|)^{3/2}}{\overline{wb}^2}\mathrm{d}\overline{wb} \approx 0. \tag{61}$$

It follows from the above expression that under the assumption $\Lambda \approx L$,

$$\left(\frac{\mathrm{d}\,\overline{wb}}{\mathrm{d}\overline{uw}}\right) \approx -\frac{3}{2}\frac{\overline{wb}}{\overline{uw}} = -\frac{3}{2}\frac{\sqrt{|\overline{uw}|}}{\kappa\Lambda}, \tag{62}$$

$$\left(\frac{\mathrm{d}\,\overline{wb}}{\mathrm{d}\overline{uw}}\right)^2 \approx \frac{9}{4}\frac{\overline{wb}^2}{\overline{uw}^2} = -\frac{9}{4}\frac{\overline{wb}}{\sqrt{|\overline{uw}|}}\frac{1}{\kappa\Lambda}. \tag{63}$$

Similar arguments apply for the ratio $\mathrm{d}\,\overline{uw}/\mathrm{d}\,\overline{w^2}$. Under the assumption $\overline{uw} \approx \overline{w^2}$ we obtain:

$$\frac{\mathrm{d}\,\overline{uw}}{\mathrm{d}\,\overline{w^2}} \approx \frac{\overline{uw}}{\overline{w^2}}. \tag{64}$$

Proceeding similarly as in Sect. 6.2, we obtain the following functional forms of S and N^2:

$$S = -\left(\frac{\mathrm{d}\overline{wb}}{\mathrm{d}\overline{uw}}\right)\left(\frac{z-z_0}{L}\right)^{\chi} F\left(\frac{\mathrm{d}\overline{uw}}{\mathrm{d}\overline{w^2}}\right), \tag{65a}$$

$$N^2 = \left(\frac{\mathrm{d}\overline{wb}}{\mathrm{d}\overline{uw}}\right)^2\left(\frac{z-z_0}{L}\right)^{\chi} H\left(\frac{\mathrm{d}\overline{uw}}{\mathrm{d}\overline{w^2}}\right), \tag{65b}$$

where we introduced the Obukhov length $L = -|\overline{uw}_0|^{3/2}/(\kappa\overline{wb}_0)$ for dimensional consistency. The definition $Ri = N^2/S^2$ now implies:

$$Ri = \frac{H}{F^2}\left(\frac{z-z_0}{L}\right)^{\chi}. \tag{66}$$

Solving Eq. (66) for $(z-z_0)/L$, and substituting back to Eqs. (65a) and (65b), we obtain:

$$S = -\left(\frac{\mathrm{d}\overline{wb}}{\mathrm{d}\overline{uw}}\right)\frac{1}{Ri}G\left(\frac{\mathrm{d}\overline{uw}}{\mathrm{d}\overline{w^2}}\right), \tag{67a}$$

$$N^2 = \left(\frac{\mathrm{d}\overline{wb}}{\mathrm{d}\overline{uw}}\right)^2\frac{1}{Ri}G^2\left(\frac{\mathrm{d}\overline{uw}}{\mathrm{d}\overline{w^2}}\right), \tag{67b}$$

where $G = H/F$. Equations (67a) and (67b) do not depend explicitly on χ.

Functions (67a) and (67b) reduce to the Monin and Obukhov (1954) scaling predictions at large stratification limit, if Eqs. (62) and (63) hold and $F = const$, $H = const$, $Ri = 0.2$. In this case, by setting $G = 2/3$, we obtain:

$$S \approx 5\frac{\sqrt{|\overline{uw}|}}{\kappa\Lambda} \approx 5\frac{u_*}{\kappa L}, \quad N^2 \approx -5\frac{\overline{wb}}{\sqrt{|\overline{uw}|}}\frac{1}{\kappa\Lambda} \approx 5\frac{b_*}{\kappa L}. \tag{68}$$

Equations (67a) and (67b) are more general than (68), because they take into account of possible variations of the fluxes and dependence on $\mathrm{d}\overline{uw}/\mathrm{d}\overline{w^2}$. However, for $G > 0$, S is positive only if $\mathrm{d}\,\overline{wb}/\mathrm{d}\,\overline{uw} < 0$. Recall the sign convention for S (cf., Eq. 62). The condition $\Lambda \simeq L$ breaks down, when the gradient $\mathrm{d}\,\overline{wb}/\mathrm{d}\,\overline{uw}$ changes its sign: this happens

with strong stratifications, as reported by Grachev et al. (2005). In this case, either of the solutions presented in Sect. 6, for the outer layer scaling should be used, or alternatively, we can consider that $\overline{wb}$ is increasing from its minimum value and change the sign in the formula (65a).

In the surface layer, where Eqs. (62) and (64), are satisfied, formulas (67a) and (67b) can be rewritten in terms of ϕ_m and ϕ_h as:

$$\phi_m \propto \frac{\xi}{Ri} G\left(\frac{\overline{uw}}{\overline{w^2}},\right), \tag{69a}$$

$$\phi_h \propto \frac{\xi}{Ri} G^2\left(\frac{\overline{uw}}{\overline{w^2}}\right). \tag{69b}$$

The resulting turbulent Prandtl number in the surface layer is not constant, but is expressed as a function of the aspect ratio, $\overline{uw}/\overline{w^2}$:

$$Pr_t = \frac{\phi_h}{\phi_m} = G\left(\frac{\overline{uw}}{\overline{w^2}}\right). \tag{69c}$$

8 Data Analysis

8.1 Estimation of Scaling Exponents

The first goal of the data analysis is to evaluate the scaling exponents, β and χ, in Eqs. (37b) and (37c). The theory does not predict their values. However, non-zero χ has implications for the scaling laws derived in Sects. 6 and 7. Note that the exponents, β and χ, should remain the same regardless of whether surface or local scaling is used.

In the analysis, we adopt a hypothetical log-linear profile as a reference, and compare it with the experimental data from SHEBA campaign (Persson et al. 2002). We expect that β and χ estimated from the SHEBA data will differ from the corresponding reference estimates, especially at large stratifications. Particularly, the estimated χ would be non-zero with strong stratifications, due to the presence of intermittency, in SHEBA data. The standard local similarity theory assumes $\chi = 0$.

The SHEBA campaign, from which data are taken from, took place from Oct 1997 to Oct 1998 on board of a Canadian icebreaker frozen into the Arctic ice pack. Turbulent fluxes and mean meteorological data were collected at five levels on a 20 m tower. Turbulent covariances available in the database are calculated with the 1-h averaging window. The measurement carried out on the Arctic offers several advantages in SBL studies over those on the mid-latitudes. During the polar night, a long-lasting SBL can be quasi stationary. Moreover, a surface covered with snow and ice is usually flat, uniform, and with no large-scale slope. Thus, data is not contaminated by katabatic flows. The data are post-processed as outlined in Grachev et al. (2005): especially, the low-frequency components of covariances are removed to filter-out the effect of gravity waves.

According to MOST, the states with non-zero stratifications are described by a sum of the linear and logarithmic profiles:

$$\frac{\bar{u}}{u_*} = \frac{1}{\kappa}\ln\left(\frac{z}{d}\right) + 5\frac{z}{L}, \quad \frac{\bar{b}}{b_*} = \frac{Pr}{\kappa}\ln\left(\frac{z}{d}\right) + 5\frac{z}{L}. \tag{70}$$

In contrast, this work predicts that the mean wind and buoyancy depend on height by power laws (cf., Eqs. 37b and 37c). They may approximate Eqs. (70) locally. Particularly, with the

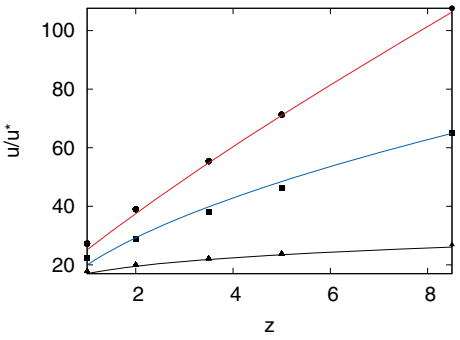

Fig. 1 Log-linear wind speeds (70) marked as symbols: $L = 0.5$ m (circles), $L = 1$ m (squares) and $L = 10$ m (triangles) and respective profiles fitted according to formula (71a) marked as curves

coefficient $\beta = 0$, the power-law solutions approach linear function as $\chi \to 0$. On the other hand, as $\chi \to -1$, the solutions approach logarithmic, as in this case $S \propto z^{-1}$ and $N^2 \propto z^{-1}$. If experimental data do not follow the log-linear profile, χ will not reach zero at large stratifications. We verify these expectations first by referring to the numerically-generated MOST solution (70) and next using experimental data of SBL.

By focusing on the surface layer, we assume that $u_0 = b_0 = 0$ in Eqs. (37b) and (37c). In this case, Eqs. (37b) and (37c) reduce to:

$$\bar{u} = C_1(z - z_0)^{1-\beta+\chi} = C_u(z - z_0)^{A_u}, \tag{71a}$$

$$\bar{b} = C_2(z - z_0)^{1-2\beta+\chi} = C_b(z - z_0)^{A_b}. \tag{71b}$$

The forms (71a), (71b) are fitted to the solution (70) locally, i.e. in the vicinity of certain height $z = z_1$, such that optimal values of β and χ are chosen. When fitting the power-law solutions (37b) and (37c) to the reference, log-linear profile, the exponents $A_u = 1 - \beta + \chi$ and $A_b = 1 - 2\beta + \chi$ in Eqs. (71a) and (71b) should change from values close to zero in the neutral state to unity in the stratified case (typically for $\xi > 1$). This is illustrated in Fig. 1, in which log-linear wind speeds (70) with $d = 10^{-4}$ m and $L = 0.5$ m, 1 m and 10 m are presented by varying symbols at five vertical levels, z. The curves fitted to Eq. (71a) are also plotted: the estimated exponents A_u are equal to 0.89, 0.73 and 0.28 for $L = 0.5$ m, 1 m and 10 m, respectively.

The same procedure can be used to analyze buoyancy profiles, and estimate the exponent A_b from Eq. (71b). Having the two exponents A_u and A_b, we can next calculate values for β and χ from the two-equation system:

$$\beta = A_u - A_b, \tag{72}$$

$$\chi = 2A_u - A_b - 1. \tag{73}$$

Since our interest here is to estimate the exponents, β and χ, and not the coefficients C_u and C_b in Eqs. (71a), (71b), we consider the ratios of respective quantities at two different heights. We also take $z_0 \approx 0$ to simplify the analysis, because our preliminary test concluded that a finite z_0 does not influence the estimates of scaling coefficients considerably. Thus, we set:

$$\frac{\bar{u}(z_i)}{\bar{u}(z_j)} = \left(\frac{z_i}{z_j}\right)^{A_u}, \quad \frac{\bar{b}(z_i)}{\bar{b}(z_j)} = \left(\frac{z_i}{z_j}\right)^{A_b}. \tag{74}$$

As a reference to compare with the observational data, we first generate the values of $\bar{u}$ and $\bar{b}$ at 5 levels, using the hypothetical "perfect" log-linear profiles as given in Eqs. (70),

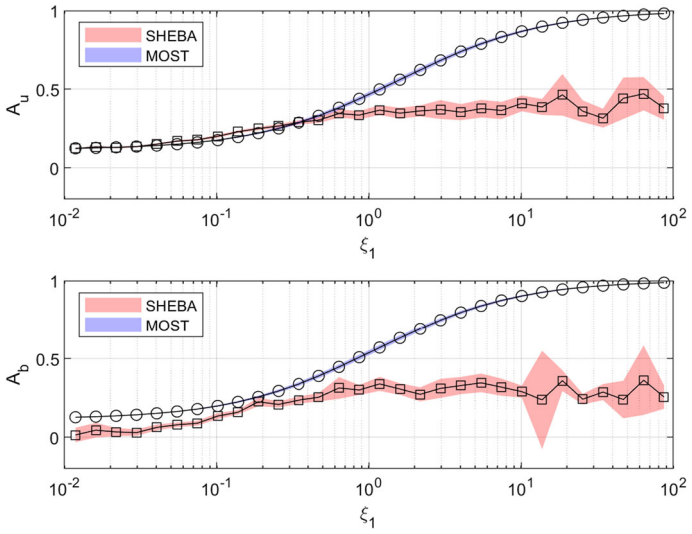

Fig. 2 Exponents **a** A_u, **b** A_b defined in Eqs. (71a) and (71b) calculated for the theoretical profile (70) (circles) and from SHEBA data (squares) together with 95% confidence intervals

i.e.,MOST data. The adopted heights are comparable to those of SHEBA instruments. We assume $d = 10^{-3}$ m and test values of L in the range $[0.1, 100]$. The data was divided into 20 logarithmically spaced bins based on the value of the similarity parameter at the first level $\xi_1 = z_1/L$. In every bin, all possible ratios of values at different vertical levels are calculated according to the formulas (74). The function $f(z) = az^p$ was fitted to these data using the nonlinear least squares algorithm in MATLAB Fitting Toolbox. We mark the fitting error based on a 95% confidence parameter in the following.

The obtained A_u and A_b values for MOST data are presented in Fig. 2 by circles. As expected, both coefficients are small with weak stratifications, where the solution is close to logarithmic and increase with the increasing stratifications towards unity as the MOST solution (70) asymptotically approaches to the linear profile.

The corresponding coefficients β and χ calculated from Eqs. (72) and (73) for MOST data are presented in Fig. 3 by circles: β remains close to zero for a full range of ξ; χ is always negative, and approaches -1 with the decreasing stratifications. As argued by Yano and Wacławczyk (2023), these solutions allow both $\bar{u}$ and $\bar{b}$ to be logarithmic in stratified flows. Here, non-zero χ does not represent the intermittency understood as alternating laminar-turbulent regimes, but merely reflects a fact that the solution (70) is a sum of two different contributions: logarithmic and linear. As the stratification increases, χ approaches 0.

In real atmospheric boundary layer flows, the solutions deviate from the MOST predictions with strong stratifications, where turbulence locally collapses (Klipp and Mahrt 2004). As a result, the coefficient χ should be smaller than the one calculated from the MOST profile Eq. (70). To investigate this possibility, we have performed an equivalent analysis for data from the SHEBA experiment. We have calculated the buoyancy based on the definition (2). Here, θ is the 1-h averaged air temperature measured at the instrument heights z_n (n =1–5); θ_0 is taken as the 1-h averaged surface temperature; θ_m is the average over the five instrument measurements.

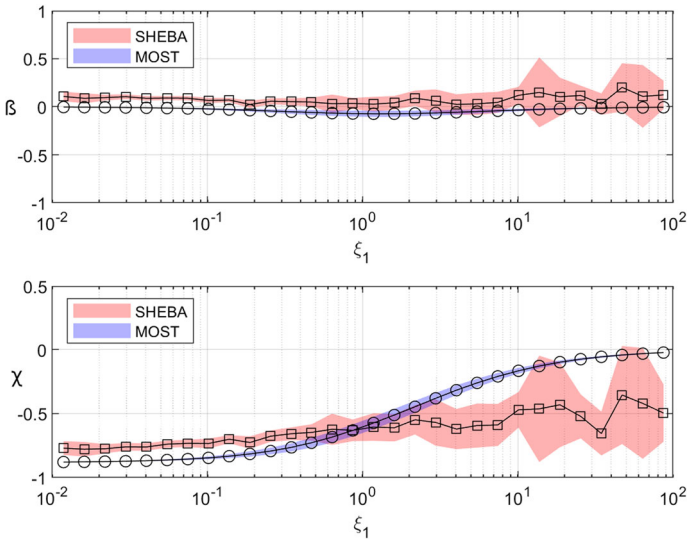

Fig. 3 Same as in Fig. 2 but for exponents β and χ calculated from Eqs. (72) and (73)

As before, the data was divided into 20 logarithmically spaced bins based on the non-dimensionalized value of the first measurement level, $\xi_1 = z_1/L$. We used the same MATLAB Fitting Toolbox to fit the data according to Eqs. (74). Resulting A_u and A_b exponents for varying ξ_1 are shown in Fig. 2 by squares. With weak stratifications, $A_u \approx 0.1$, and with increasing ξ_1, A_u increases to approximately 0.4. It does not reach the value of 1 predicted by the MOST. With very weak stratifications, $\xi_1 \sim 10^{-2}$, the estimated A_b exponent becomes close to zero. In this case, calculating a gradient of temperature becomes difficult, as the temperature varies only weakly with height. As ξ_1 increases, A_b also increases towards 0.3–0.4. Here again, deviation of the profile from the MOST solution (70) is visible: both A_u and A_b start to deviate from the theoretical predictions at ξ_1 in the range between 10^{-1} and 10^0. According to Grachev et al. (2005), it is the range where the buoyancy flux $\overline{wb}$ start to increase with height.

Corresponding β and χ values are plotted in Fig. 3: β remains close to zero for a full range of ξ_1, whereas $\chi \approx -0.8$ towards the weak stratifications, and it tends to increase with increasing ξ_1, although it is not easy to draw a definite conclusion from Fig. 3 due to the large uncertainty in the estimates. Nevertheless, it is evident that for $\xi_1 > 1$, χ estimated from the SHEBA data is significantly smaller than MOST data assuming the profile (70). We interpret it as a result of global intermittency, in which turbulence has a tendency to form layers with smaller gradients of mean wind and buoyancy than predicted by MOST.

8.2 Estimation of ϕ_m and ϕ_h and Pr_t

Next, we verify the prediction (69c) on the turbulent Prandtl number. According to Eq. (69c), this non-dimensional parameter is not constant, not as predicted by MOST, but it is a function of $\overline{uw}/\overline{w^2}$ or time. Unfortunately, the time dependence, $(t - t_0)\overline{wb}/\overline{uw}$, is difficult to investigate with only one-hourly data available. The Pr_t-dependence on the ratio, $\overline{uw}/\overline{w^2}$, is plotted in Fig. 4: it increases with the increasing $\overline{uw}/\overline{w^2}$. To investigate how the

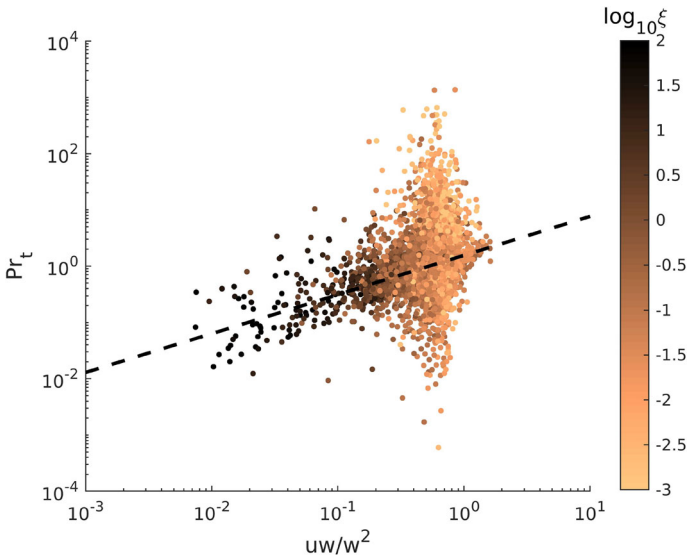

Fig. 4 Pr_t as a function of $\overline{uw}/\overline{w^2}$. Color coded is the logarithm $\log_{10}(\xi)$

argument changes with stratification, we also color-code the logarithm of non-dimensional height, $\ln(\xi)$, in this figure, where $\xi = z/L$. Small $\overline{uw}/\overline{w^2}$ tends to correspond to large ξ. As ξ decreases, the parameter $\overline{uw}/\overline{w^2}$ increases towards the value 0.9 at neutral conditions; Pr_t decreases with increasing stratifications, which was also confirmed in an earlier study by Sorbjan and Grachev (2010). Those authors plotted Pr_t calculated from SHEBA data as a function of Ri. Larger scatters of Pr_t with weaker stratifications stem from the increasing difficulties in estimating gradients of temperature and temperature fluxes in this limit.

We further verify the formulas (69a, 69b) rewritten here for clarity:

$$\phi_m = \frac{\xi}{Ri} G\left(\frac{\overline{uw}}{\overline{w^2}}\right), \quad \phi_h = \frac{\xi}{Ri} G^2\left(\frac{\overline{uw}}{\overline{w^2}}\right). \tag{75}$$

Assumptions needed to arrive at (75) are that $\Lambda \approx const$ and $\mathrm{d}\overline{uw}/\mathrm{d}\overline{w^2} \approx const$, so that $\mathrm{d}\overline{uw}/\mathrm{d}\overline{w^2} \approx \overline{uw}/\overline{w^2}$. Formulas (75) should remain true also with non-zero parameter χ. The dependence of Pr_t on $\overline{uw}/\overline{w^2}$, as defined as a function, G, by Eq. (69c), was roughly estimated from Fig. 4 as $G \approx 1.1(\overline{uw}/\overline{w^2})^{0.7}$

In Figs. 5 and 6, we plot ϕ_m and ϕ_h against the right-hand sides of Eqs. (75). All terms are calculated from the SHEBA data for all measurement levels. The predictions of Eq. (75) are plotted as solid lines. Data points corresponding to larger stratifications follow the predictions more closely than those of smaller ξ. However, some of the points clearly follow a different power laws, marked by dashed lines on both plots, which are defined by:

$$\phi_m \propto \left(\frac{\xi}{Ri} G\right)^{1/3}, \quad \phi_h \propto \left(\frac{\xi}{Ri} G^2\right)^{-1}. \tag{76}$$

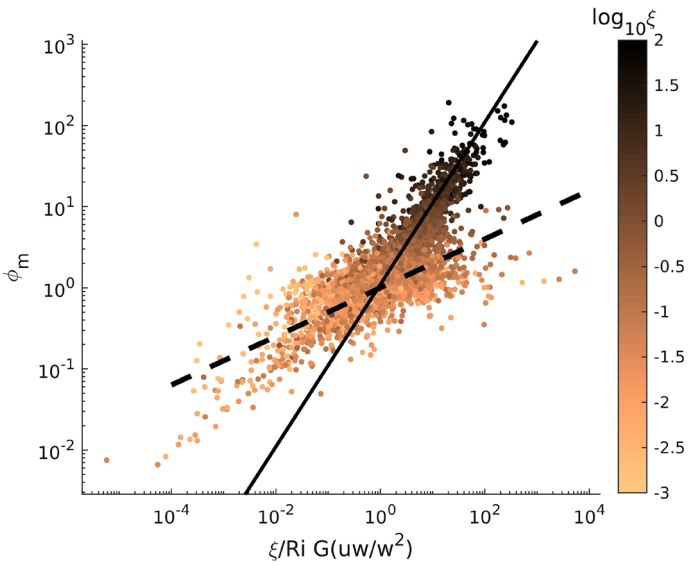

Fig. 5 ϕ_m as a function of ξ/RiG. SHEBA data: symbols, predictions (75): solid line, predictions (76): dashed line. Color coded is the logarithm $\log_{10}(\xi)$

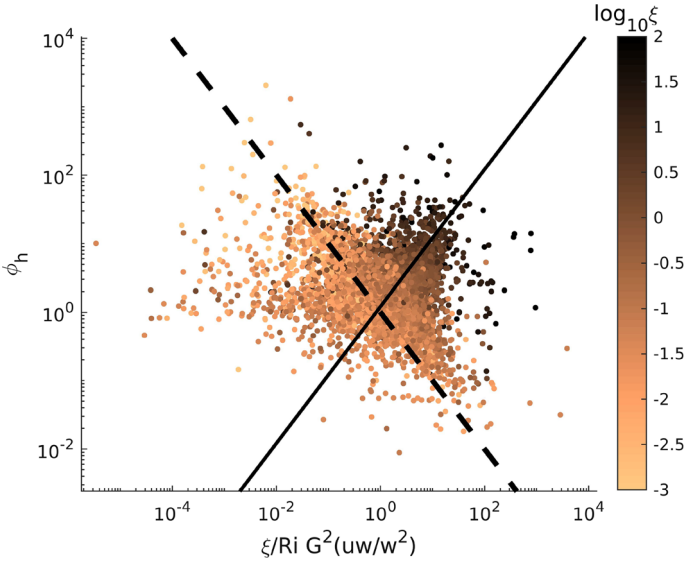

Fig. 6 ϕ_h as a function of ξ/RiG^2. SHEBA data: symbols, predictions (75): solid line, predictions (76): dashed line. Color coded is the logarithm $\log_{10}(\xi)$

These power laws actually correspond to logarithmic solutions for $G \approx const$, which can be verified after substituting definitions of $\phi_m, \phi_h, \xi = z/L$ and Ri into (76):

$$N^2 \equiv \frac{d\bar{b}}{dz} \sim \frac{b_*}{\kappa z}, \quad S \equiv \frac{d\bar{u}}{dz} \sim \frac{u_*}{\kappa z}. \tag{77}$$

The formula (76) is consistent with (75) when $z/L \sim Ri$. The former condition is not fulfilled exactly with weak stratifications due to large relative errors of $\overline{wb}$ and N^2, resulting in large estimation uncertainties of Ri and L. In this regime, the solutions still follow the scaling (76), which is satisfied by the logarithmic function, in spite of the errors in estimating L and Ri. Also note that the relations (76) do not result directly from the Lie group analysis, but they are rather considered a generalization of Eq. (75). Other possible reasons for the deviations in Figs. 5 and 6 is that the assumption of $\Lambda \approx const$ may no longer be satisfied with very strong stratifications, where a scatter of data is also considerable. Variability of $\mathrm{d}\overline{uw}/\mathrm{d}\overline{w^2}$ may also contribute to the observed deviations.

9 Conclusions

In this work, we have shown that the local similarity theories of ABL can be derived by analysis of a governing set of equations in invariant Lie-group forms, for example, given by Eq. (29) for the heat equation (16). Our investigation also takes into account of a possible presence of intermittency due to a local collapse of turbulence (Ansorge and Mellado 2014).

We have examined the two different regimes of ABL by adopting the two different approaches. First, we have assumed that the buoyancy and momentum fluxes follow the outer-layer scaling, and increase with height from negative values close to the surface towards zero at $z = h$. The characteristic length scale, h, has been taken as the ABL height. The derived solutions, (46a, 46b), for the non-dimensional similarity functions, ϕ_m and ϕ_h, are not universal, since they contain the intermittency parameter χ, which cannot be determined *a priori*, and is constant only locally. On the other hand, the turbulent Prandtl number, Pr_t, in the invariant form, Eq. (47), obtained from the ratios between the two similarity functions, ϕ_m and ϕ_h, does not depend on χ. Yet, the form also predicts that the turbulent Prandtl number, Pr_t, is not constant, either, but depend on the ratio of the Reynolds stresses, $\overline{uw}/\overline{w^2}$, or alternatively, the non-dimensional time, $(t - t_0)\,\overline{wb}/\overline{uw}$. Identifying these two invariants as arguments of the similarity functions is remarkable, especially considering an adopted truncation of the system into the mean momentum and buoyancy prognostic equations. The ratio, $\overline{uw}/\overline{w^2}$, may be considered a measure of flow anisotropy, or alternatively to be an aspect ratio of eddies. Furthermore, the same dependency can be re-interpreted in terms of a transiency of the system. This further suggests an intimate link between the transiency and the anisotropy of the flows. We have also demonstrated that our solutions reduce to the gradient-based similarity theory by Sorbjan (2006) by setting $\chi = 0$.

In the second approach, we have considered the surface-layer scaling, in which the fluxes vary only little with height. Typically, close to the surface, $\overline{uw}$ will increase with height, and $\overline{wb}$ will decrease with increasing $\xi = z/L$. No external length scale is introduced in this case. We obtain relations for S and N^2 as functions of vertical gradients of fluxes, as in Eqs. (67a) and (67b): they are key results from Sect. 7. When dependence on $\mathrm{d}\overline{uw}/\mathrm{d}\overline{w^2}$ and a contribution of the intermittency is neglected, derived functions reduce to the common scaling $\phi_m \propto \xi$ and $\phi_h \propto \xi$, predicted by Monin and Obukhov (1954) for large stratifications.

A goal of data analysis in Sect. 8 has been to estimate values of exponents β and χ found in the identified invariant solutions, Eqs. (37a)–(37g), for a full set of both independent and dependent variables of the boundary-layer system under considerations. We have compared the data from the SHEBA experiment against the theoretical log-linear profiles (70) predicted from MOST. The coefficient, χ, estimated for the theoretical profiles (70) increases from -1 at small $\xi = z/L$ to zero towards large ξ, over which the solution is purely linear. On the other hand, the coefficient χ estimated from SHEBA data levels-off at around -0.5. This confirms that both the wind shear and the stratification are predicted by algebraic scaling laws (40a) and (40b). A difference between the MOST and experiment increases with the increasing ξ; it can be attributed to the presence of global intermittency, which is quantified in our analysis by a non-zero parameter, χ.

In Sect. 8.2, we have further investigated the validity of the similarity solutions for ϕ_m, ϕ_h and Pr_t in the surface layer, as derived as Eqs. (69a, b, c). As predicted, the turbulent Prandtl number, Pr_t, is not constant, but depends on the measure, $\overline{uw}/\overline{w^2}$, of the anisotropy. Interestingly, data with stronger stratifications follows the predictions of Eqs. (69a, b) for ϕ_m and ϕ_h quite closely, whereas for the smaller non-dimensional height, $\xi = z/L$, data rather follows the scalings $\phi_m \propto (\xi/RiG)^{1/3}$ and $\phi_h \propto (\xi/RiG^2)^{-1}$: these forms correspond to logarithmic solutions when $G \approx const$.

There exist various intriguing directions for further studies based on the symmetries of the ABL flows. First, the identified time dependence on solutions (cf., Eq. 42) in this study requires further attentions. Second, the outer-layer scaling investigated in Sect. 6 and the role of exponent χ should be investigated in more detail based on experimental data and by comparison with existing analyses, e.g.,Allouche et al. (2022). Hopefully, derived invariant functions will improve parametrizations of the stable atmospheric boundary layers and provide the basis for turbulence closures which account for the intermittent structure of ABL, such as the stochastic model by Allouche et al. (2021). Finally, the effect of Coriolis force and the resulting modification of symmetries should be accounted for. This may improve predictions at very large stratifications, where the ABL height is relatively small, and the statistics of the whole ABL are influenced by the Earth's rotation.

Acknowledgements The financial support of the National Science Centre, Poland (Project No. 2020/37/B/ST10/03695) is gratefully acknowledged. JIY further acknowledges support of IDUB Mentoring Programm of the University of Warsaw.

Data availability The datasets analysed during this study are available in the repository of the Earth Observing Laboratory: https://data.eol.ucar.edu/project/SHEBA Post-processed data were made available to us by A. Grachev after our request.

References

Allouche M, Bou-Zeid E, Ansorge C, Katul GG, Chamecki M, Acevedo O, Thanekar S, Fuentes JD (2022) The detection, genesis, and modeling of turbulence intermittency in the stable atmospheric surface layer. J Atmos Sci 79:1171–1190

Allouche M, Katul GG, Fuentes JD, Bou-Zeid E (2021) Probability law of turbulent kinetic energy in the atmospheric surface layer. Phys Rev Fluids 6:074601

Ansorge C, Mellado JP (2014) Global intermittency and collapsing turbulence in the stratified planetary boundary layer. Boundary-Layer Meteorol 153:89–116

Araya G, Castillo L, Hussain F (2015) The log behaviour of the Reynolds shear stress in accelerating turbulent boundary layers. J Fluid Mech 775:189–200

Avsarkisov V, Hoyas S, Oberlack M, García-Galache J (2014) Turbulent plane Couette flow at moderately high Reynolds number. J Fluid Mech 751:R1

Barenblatt GI (1996) Scaling, self-similarity, and intermediate asymptotics. Cambridge University Press, Cambridge

Bluman GW, Kumei S (1989) Symmetries and differential equations. Springer-Verlag, New York

Buckingham E (1914) On physically similar systems; illustrations of the use of dimensional equations. Phys Rev 4:345

Businger JA, Wyngaard JC, Izumi Y, Bradley EF (1971) Flux-profile relationships in the atmospheric surface layer. J Atmos Sci 28:181–189

Foken T (2006) 50 years of the Monin–Obukhov similarity theory. Boundary-Layer Meteorol 119:431–447

Frewer M, Khujadze G, Foysi H (2015) Comment on statistical symmetries of the Lundgren–Monin–Novikov hierarchy. Phys Rev E 92:067001

Grachev AA, Fairall CW, Persson PO, Andreas EL, Guest PS (2005) Stable boundary layer scaling regimes: the SHEBA data. Boundary-Layer Meteorol 116:201–235

Grachev AA, Andreas EL, Fairall CW et al (2013) The critical Richardson number and limits of applicability of local similarity theory in the stable boundary layer. Boundary-Layer Meteorol 147:51–82

Grachev AA, Andreas EL, Fairall CW, Guest PS, Persson POG (2015) Similarity theory based on the Dougherty–Ozmidov length scale. Q J R Meteorol Soc 141:1845–1856

Ji Y, She ZS (2021) Analytic derivation of Monin–Obukhov similarity function for open atmospheric surface layer. Sci China Phys Mech Astron 64:34711

Katul GG, Banerjee T, Cava D, Germano M, Porporato A (2016) Generalized logarithmic scaling for high-order moments of the longitudinal velocity component explained by the random sweeping decorrelation hypothesis. Phys Fluids 28:095104

Khujadze G, Oberlack M (2004) DNS and scaling laws from new symmetry groups of ZPG turbulent boundary layer flow. Theor Comput Fluid Dyn 18:391–411

Klipp CL, Mahrt L (2004) Flux-gradient relationship, self-correlation and intermittency in the stable boundary layer. Q J R Meteorol Soc 130:2087–2103

Lighthill K (1978) Waves in fluids. Cambrdge University Press, Cambridge

Łobocki L (2013) Analysis of vertical turbulent heat flux limit in stable conditions with a local equilibrium, turbulence closure model. Boundary-Layer Meteorol 148:541–555

Łobocki L, Porretta-Tomaszewska P (2021) Prediction of gradient-based similarity functions from the Mellor–Yamada model. Q J R Meteorol Soc 147:3922–3939

Monin AS, Obukhov AM (1954) Basic laws of turbulent mixing in the surface layer of the atmosphere. Tr Nauk SSSR Geophiz Inst 24:163–187 (**in Russian: translation available eg. at:** https://mcnaughty.com/keith/papers/Monin_and_Obukhov_1954.pdf)

Nieuswtadt FTM (1984) The turbulent structure of the stable, nocturnal boundary layer. J Atmos Sci 41:2202–2216

Oberlack M (2001) A unified approach for symmetries in plane parallel turbulent shear flows. J Fluid Mech 427:299–328

Oberlack M, Rosteck A (2010) New statistical symmetries of the multi-point equations and its importance for turbulent scaling laws. Discrete Contin Dyn Syst S3:451–471

Oberlack M, Hoyas S, Kraheberger SV, Alcántara-Ávila F, Laux J (2022) Turbulence statistics of arbitrary moments of wall-bounded shear flows: a symmetry approach. Phys Rev Lett 128:024502

Obukhov AM (1948) Turbulence in an atmosphere with a non-uniform temperature. Trans Inst Theor Geophys 1:95–115 (**in Russian: translation in Boundary Layer Meteorol 2 (1971), 7–29**)

Persson POG, Fairall CW, Andreas EL, Guest PS, Perovich DK (2002) Measurements near the atmospheric surface flux group tower at SHEBA: near-surface conditions and surface energy budget. J Geophys Res 107:8045

Pukhnachev VV (1972) Invariant solutions of Navier–Stokes equations describing motions with free boundary. Dokl Akad Nauk 202:302
Rosteck A (2014) Scaling laws in turbulence—a theoretical approach using Lie-point symmetries. PhD Thesis, TU Darmstadt, Germany
Sadeghi H, Oberlack M, Gauding M (2021) New symmetry-induced scaling laws of passive scalar transport in turbulent plane jets. J Fluid Mech 919:A5
Sorbjan Z (1989) Structure of the atmospheric boundary layer. Prentice Hall, Englewood Cliffs
Sorbjan Z (2006) Local structure of stably stratified boundary layer. J Atmos Sci 63:1526–1537
Sorbjan Z (2010) Gradient-based scales and similarity laws in the stable boundary layer. Q J R Meteorol Soc 136:1243–1254
Sorbjan Z (2012) The height correction of similarity functions in the stable boundary layer. Boundary-Layer Meteorol 142:21–31
Sorbjan Z (2016) Similarity scaling system for stably stratified turbulent flows. Q J R Meteorol Soc 142:805–810
Sorbjan Z, Grachev AA (2010) An evaluation of the flux-gradient relationship in the stable boundary layer. Boundary-Layer Meteorol 135:385–405
Stiperski I, Calaf M (2023) Generalizing Monin–Obukhov similarity theory (1954) for complex atmospheric turbulence. Phys Rev Lett 130:124001
Stiperski I, Chamecki M, Calaf M (2021) Anisotropy of unstably stratified near-surface turbulence. Boundary-Layer Meteorol 180:363–384
Wacławczyk M, Staffolani N, Oberlack M, Rosteck A, Friedrich R (2014) Statistical symmetries of the Lundgren–Monin–Novikov hierarchy. Phys Rev 90:013022
Wacławczyk M, Grebenev VN, Oberlack M (2017) Lie symmetry analysis of the Lundgren–Monin–Novikov equations for multi-point probability density functions of turbulent flow. J Phys A Math Theor 50:175501
Yano JI, Bonazzola M (2009) Scale analysis for large-scale tropical atmospheric dynamics. J Atmos Sci 66:159–172
Yano J, Wacławczyk M (2022) Nondimensionalization of the atmospheric boundary-layer system: Obukhov length and Monin–Obukhov similarity theory. Boundary-Layer Meteorol 182:417–439
Yano J, Wacławczyk M (2023) Symmetry invariant solutions in atmospheric boundary layers. J Atmos Sci 81:263–277
Zilitinkevich S, Calanca P (2000) An extended similarity-theory for the stably stratified atmospheric surface layer. Q J R Meteorol Soc 126:1913–1923
Zilitinkevich S, Esau IG (2005) Resistance and heat-transfer for stable and neutral planetary boundary layers: old theory advanced and re-evaluated. Q J R Meteorol Soc 131:1863–1892
Zilitinkevich SS, Esau IN (2007) Similarity theory and calculation of turbulent fluxes at the surface for the stably stratified atmospheric boundary layer. Boundary-Layer Meteorol 125:193–205